

Supporting Information

Identifying trends and descriptors for selective CO₂ conversion to CO over transition metal carbides

*Marc D. Porosoff, Shyam Kattel, Wenhui Li, Ping Liu, and Jingguang G. Chen**

Table of Contents

1. Catalyst Preparation	S2
2. X-ray Diffraction (XRD)	S2
3. Density Functional Theory (DFT)	S2
4. X-ray Absorption Spectroscopy (XAS)	S4
5. Reactor Studies	S4
6. References	S5

1. Catalyst Preparation

Mo₂C was synthesized by carburization of MoO₃ at 850 °C, following a procedure outlined in Kimmel et al.¹ NbC was prepared through direct carburization of Nb₂O₅ at 1000°C in 21 % CH₄ in H₂. All catalysts were reduced in a 50% H₂ in He mixture prior to reaction.

2. X-ray Diffraction (XRD)

X-ray diffraction (XRD) measurements of the transition metal carbides were performed on a PANalytical X'Pert X-ray diffractometer using Cu K α radiation, operated at 45 kV and 40 mA over the range of $2\theta = 30.0\text{--}80.0^\circ$. Powder catalysts were transferred into the instrument as-is.

3. Density Functional Theory (DFT)

Spin polarized periodic density functional theory (DFT)^{2, 3} calculations were performed using Vienna *Ab-initio* Simulation Package (VASP) code.^{4, 5} A plane wave cut-off energy of 400 eV and 3 \times 3 \times 1 Monkhorst-Pack⁶ grid were used for total energy calculations. The interactions between electrons and nuclei were treated with all electron like projector augmented wave (PAW) potentials with the generalized gradient approximation (GGA)^{7, 8} using PW91 functionals.⁹ Ionic positions were optimized until Hellman-Feynman force on each ion was smaller than 0.02 eV \AA^{-1} .

Transition metal terminated-transition metal carbide (TMC) surfaces were modeled using a 3 \times 3 surface slab cell with four bilayers (a bilayer contains a unit of one TM layer and one C layer) of atoms, Fig. 1. A vacuum layer of ~ 12 \AA thick was added in the slab cell along the direction perpendicular to the surface in order to avoid the artificial interactions between the surface and

its periodic images. During geometry optimization, atoms in the top two bilayers were allowed to relax while the atoms in the bottom two bilayers were fixed. The binding energy of oxygen (BEO) was calculated as $BEO = E(\text{slab}+\text{O}) - E(\text{slab}) - 1/2E(\text{O}_2)$, where $E(\text{slab}+\text{O})$, $E(\text{slab})$ and $E(\text{O}_2)$ were the total energies of slab with adsorbed O, clean slab and gas phase O_2 molecule, respectively. The transition states of chemical reactions were located using the dimer method.¹⁰

Table 1 Atomic oxygen binding energy (BEO in eV) on transition metal terminated transition metal carbide surfaces. Bold number on each surface represents the energetically most stable site.

(111) surface					(0001) surface			
site	TiC	ZrC	NbC	TaC	site	$\beta\text{-Mo}_2\text{C}$	site	WC
fcc	-5.74	-6.12	-4.66	-4.79	fcc	-4.71	hollow	-3.78
hcp	-4.92	-5.29	-4.69	-4.73	hcp-1	-4.00	hcp	-4.72
top	-3.52	-3.39	-3.23	-3.10	hcp-2	-4.31	top	-2.41
bridge	NS	NS	NS	NS	hcp-3	-4.68	bridge	NS
					top	-3.11		
					bridge-1	NS		
					bridge-2	NS		

NS=not stable

Table 2 Reaction energetics (in eV) on the TiC(111) surface.

Reactions	Activation energy (E_a)	Reaction energy (ΔE)
$^*\text{H}_2 \rightarrow ^*\text{H} + ^*\text{H}$	0	--
$^*\text{O} + ^*\text{H} \rightarrow ^*\text{OH}$	2.54	1.82
$^*\text{OH} + ^*\text{H} \rightarrow ^*\text{H}_2\text{O}$	3.21	3.15
$^*\text{OH} + ^*\text{OH} \rightarrow ^*\text{OH} + ^*\text{H}$	1.41	1.25
$\text{H}_2(\text{g}) + ^*\text{O} \rightarrow ^*\text{OH} + ^*\text{H}$	1.15	-0.61

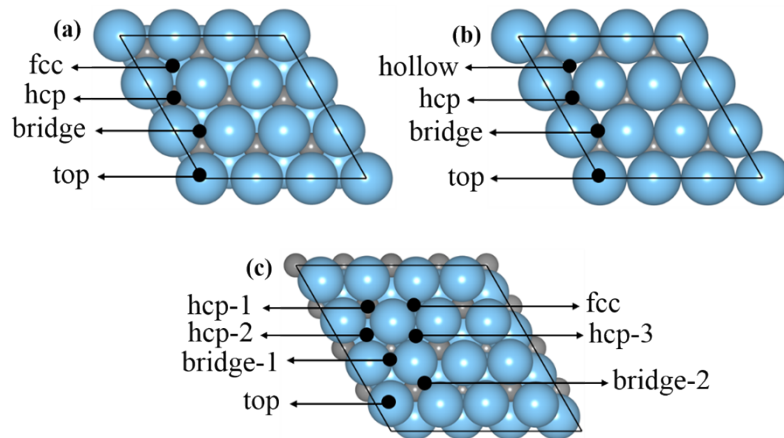


Fig. 1 Various surface adsorption sites on (a) TM terminated TMC(111) (TM=Ti, Zr, Nb and Ta), (b) W terminated WC(0001) and (c) Mo terminated $\beta\text{-Mo}_2\text{C}$ (0001) surfaces. Light blue balls represent transition metal atoms and grey balls represent carbon atoms.

4. X-ray Absorption Near Edge Spectroscopy (XANES)

X-ray absorption near edge spectroscopy (XANES) measurements confirmed the oxidation state of Mo₂C and TiC catalysts. XANES measurements were performed on the X18B beamline at the National Synchrotron Light Source (NSLS), Brookhaven National Laboratory. Catalyst samples were diluted with boron nitride, pressed into a pellet, then grinded and sieved (100-150 mesh). The mass of the catalyst and dilution were determined so the sample amount was two absorption lengths to maximize the signal to noise ratio of each sample. Mo and Ti K-edge XANES spectra were recorded for Mo₂C and TiC catalysts under the same procedure. Initial spectra were recorded at room temperature and after reduction in H₂ and He at 723 K. Following reduction, the sample was treated with a 1:2 CO₂:H₂ gas mixture, to mirror reactor studies, and then in pure CO₂ to confirm the oxidation of carbides by the partial dissociation of CO₂. During each gas treatment, the *in-situ* cell was heated at 573 K for 60 minutes, and then cooled to room temperature before collecting XANES measurements. The XANES spectrum for Mo₂C from each treatment condition was fitted by a linear combination of MoO₃, MoO₂ and Mo₂C standards, by using the linear combination fit feature in Athena (IFEFFIT 1.2.11 data analysis package).

5. Reactor Studies

CO₂ reduction was carried out in a quartz U-tube reactor under atmospheric pressure. In each experiment, approximately 100 mg catalyst (60-80 mesh) was loaded into the flow reactor. Before the reaction, the catalyst was reduced under a 1:1 hydrogen and helium mixture (50 mL/min total flow) at 723 K for 1 h. To start the reaction, the flow of CO₂ and hydrogen were set at 20 mL/min and 40 mL/min, respectively. For each experiment, the temperature was raised to 573 K and the reaction was run for approximately 8 hours. Product streams were analyzed by online gas chromatography equipped with a flame ionization detector (FID) and thermal conductivity detector (TCD). The concentration of each gas-phase species was calibrated by correlating the peak area of the pure compound to its concentration in a calibration gas standard.

6. References

1. Y. C. Kimmel, X. Xu, W. Yu, X. Yang and J. G. Chen, *ACS Catal.*, 2014, **4**, 1558-1562.
2. P. Hohenberg and W. Kohn, *Phys. Rev.*, 1964, **136**, B864-B871.
3. W. Kohn and L. J. Sham, *Phys. Rev.*, 1965, **140**, A1133-A1138.
4. G. Kresse and J. Furthmüller, *Comp. Mat. Sci.*, 1996, **6**, 15-50.
5. G. Kresse and J. Hafner, *Phys. Rev. B*, 1993, **48**, 13115-13118.
6. H. J. Monkhorst and J. D. Pack, *Phys. Rev. B*, 1976, **13**, 5188-5192.
7. G. Kresse and D. Joubert, *Phys. Rev. B*, 1999, **59**, 1758-1775.
8. P. E. Blöchl, *Phys. Rev. B*, 1994, **50**, 17953-17979.
9. J. P. Perdew and Y. Wang, *Phys. Rev. B*, 1992, **45**, 13244-13249.
10. G. Henkelman and H. Jónsson, *J. Chem. Phys.*, 1999, **111**, 7010-7022.